# Remediation of diethyl phthalate in aqueous effluents with tio2-supported rh0 nanoparticles as multicatalytic materials

Audrey Denicourt-Nowicki, C.-H. Pélisson, I. Soutrel, L. Favier, Alain Roucoux

catalysts

MDPI

*Article*

# Remediation of Diethyl Phthalate in Aqueous Effluents with $TiO_2$-Supported Rh0 Nanoparticles as Multicatalytic Materials

**Audrey Denicourt-Nowicki *, Carl-Hugo Pélisson, Isabelle Soutrel, Lidia Favier and Alain Roucoux ***

Univ Rennes, Ecole Nationale Supérieure de Chimie de Rennes, CNRS, ISCR-UMR 6226, F-35000 Rennes, France; carl.pelisson@gmail.com (C.-H.P.); isabelle.soutrel@ensc-rennes.fr (I.S.); lidia.favier@ensc-rennes.fr (L.F.)
* Correspondence: Audrey.Denicourt@ensc-rennes.fr (A.D.-N.); alain.roucoux@ensc-rennes.fr (A.R.)

**Abstract:** An innovative "domino" process, based on an arene hydrogenation followed by a photocatalytic step, was designed for the remediation of endocrine disrupting compounds, in highly concentrated aqueous effluents. The novelty relies on the use of $TiO_2$-supported zerovalent Rh nanoparticles as multicatalytic materials (MCMs) for this two-step treatment, applied on diethyl phthalate, which is a model aromatic pollutant frequently present in aquatic environments. This nanocomposite advanced material, which was easily prepared by a green, wet impregnation methodology, proved to be active in the successive reactions, the reduction in the aromatic ring, and the photodegradation step. This sustainable approach offers promising alternatives in the case of photoresistive compounds.

**Keywords:** diethyl phthalate; domino process; remediation; multicatalytic materials; nanoparticles



**Citation:** Denicourt-Nowicki, A.; Pélisson, C.-H.; Soutrel, I.; Favier, L.; Roucoux, A. Remediation of Diethyl Phthalate in Aqueous Effluents with $TiO_2$-Supported Rh0 Nanoparticles as Multicatalytic Materials. *Catalysts* **2021**, *11*, 1166. https://doi.org/10.3390/catal11101166

Academic Editor: Antonio Eduardo Palomares

Received: 26 August 2021
Accepted: 23 September 2021
Published: 27 September 2021



## 1. Introduction

Owing to their intensive use as plasticizers in polyvinyl chloride plastics, or as additives in personal care products or printing inks, and with a world production of several million tons per year [1,2], phthalate esters (PAEs) are present at very high concentrations in many surface waters and sediments [3,4]. These ubiquitous pollutants are known as endocrine disruptors [5,6] and/or suspected as carcinogenic compounds [7,8]. The release, and the persistent presence in water and wastewater of these PAEs, considered as priority pollutants by the United States Environmental Protection Agency (US EPA) and some of its international counterparts [9], have become a societal concern over the past few years.

In that context, the development of fast and efficient treatment processes for the remediation of these harmful endocrine disrupting compounds is highly required. Various approaches have been used to improve the removal of phthalates during water treatment, including biotransformation [10,11], adsorption [12–14], and advanced oxidation processes [15–17]. Although the biodegradation of phthalates by activated sludges has been demonstrated, under either aerobic or anaerobic conditions [18,19], this approach still suffers from long reaction times to transform these pollutants into harmless compounds, as well as incomplete degradation. In the same way, adsorptive removal proves to be effective for PAEs remediation, but presents high costs and requires further treatment. Finally, advanced oxidation processes (AOPs) have been considered as pertinent methodologies to remove phthalates from wastewaters [20,21], including the photochemically enhanced Fenton reaction [22,23], the combinations of $TiO_2$ or $H_2O_2$ with ultraviolet (UV) light irradiation [20,24], ozonation reactions [25,26], and catalytic ozonation processes [27–29].

Among the various oxidation approaches [30], $TiO_2$-mediated photocatalytic decomposition is considered as a relevant technology to convert complex organic pollutants present in water into simple, non-toxic, and environmentally acceptable constituents [31–34], ideally carbon dioxide and water [35]. The key advantages of this methodology include its operation at ambient conditions, as well as the use of an inexpensive, commercially available, and photochemically stable catalyst [36]. Some examples of the photocatalyzed degradation of

phthalates have been reported with aqueous suspensions of titanium dioxide [37,38], $TiO_2$ pillared montmorillonites [39], or titania-coated magnetic composites [40,41]. Moreover, doping through incorporation or decoration with transition metal cations or noble metals has also been reported to extend the spectra response of this photocatalytic material to the visible region, and thus to achieve higher photocatalytic activity [42–44]. In the last decades, nanometer-sized particles have been considered as pertinent and green catalysts, owing to their unique surface properties, thus affording relevant activities and original selectivities [45]. In that context, we have developed the eco-responsible synthesis of aqueous suspensions of metal nanoparticles as active catalytic species, [46,47] and their easy deposition without a calcination step on various supports, including $TiO_2$ [48].

In the drive towards alternative and faster wastewater treatments, we describe a "domino" process [49] (Figure 1), based on hydrogenation of the aromatic structure of diethyl phthalate into hydrocarbons, as saturated and less toxic products, which could then be converted into $CO_2$ and $H_2O$ through a photocatalytic step, using a single composite material, by co-immobilization of two catalytic species within the same matrix. For that purpose, zerovalent rhodium nanoparticles (NPs), which are known to be active in the reduction in aromatic rings under mild conditions [50], are deposited on a $TiO_2$ anatase support, which is the most often used photocatalyst, due to its relevant activity, high stability, non-environmental impact, and low cost. The feasibility of this wastewater treatment was investigated on diethyl phthalate (DEP), an aromatic endocrine disrupting compound, using Rh(0)NPs@$TiO_2$ as the sole catalytic material, combining two different catalytic properties for these successive molecular transformations [43]. This short-chained phthalate [51], which has been frequently identified in diverse aquatic environments [52,53], owing to its easy leaching from plastics [54], is among the most highly suspected endocrine disrupting compounds that interfere with the hormonal system of wildlife [15]. Obviously, this two-step treatment process will be particularly adapted for the removal of phthalates in low volumes of aqueous effluents, but also in high concentrations, more particularly, wastewaters coming from the plasticizer industry or vat bottom residues (~200 $mg \cdot L^{-1}$).

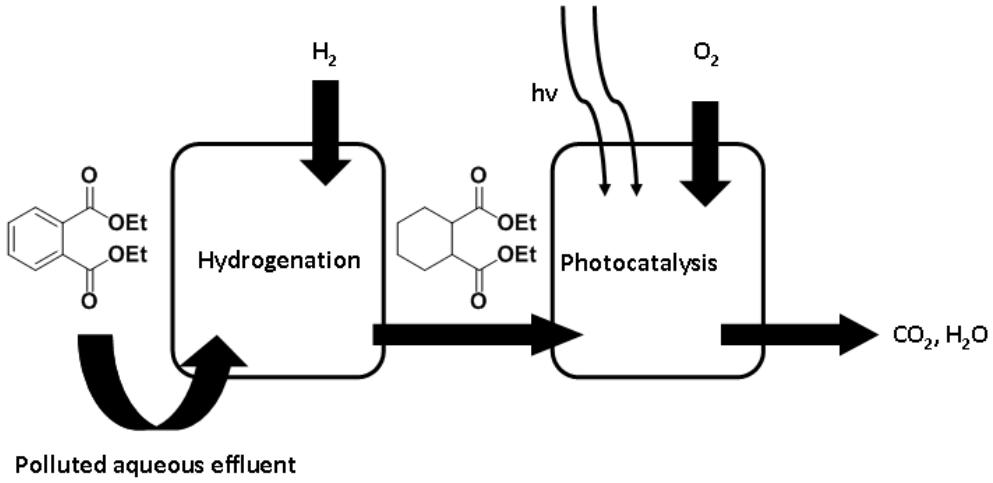


**Figure 1.** Removal of diethyl phthalate (DEP) through a pertinent "domino" process.

## 2. Results and Discussion

Rh(0)NPs supported on $TiO_2$ anatase were easily synthesized by a sustainable methodology, based on the wet impregnation of the inorganic active matrix, by an aqueous suspension of rhodium (0) colloids under mild conditions, in air, without any drastic treatments, such as calcination [48,55]. The *N*,*N*-dimethyl-*N*-cetyl-*N*-(2-hydroxyethyl) ammonium chloride (HEA16Cl)-prestabilized rhodium NPs, [56] fully characterized and possessing sizes of around 2.4 nm, [57,58], were easily deposited on the titania photocatalytic support, as shown by the color change from black to colorless. After filtration, the multicatalytic material was washed several times with water and dried overnight (Figure 2). The metal

loading, which was determined by inductively coupled plasma (ICP) analysis, was around 0.09 wt.%, as expected. The presence of Rh(0) NPs possessing an average size of 3–4 nm, very close to the size of anatase, was checked by high-resolution transmission electron microscopy (HRTEM micrograph Figure 3a—contrasted zone) and confirmed by energy-dispersive X-ray (EDX) spectrometry (Rh signals at 2.696 and 2.834 keV in Figure 3c) [55].

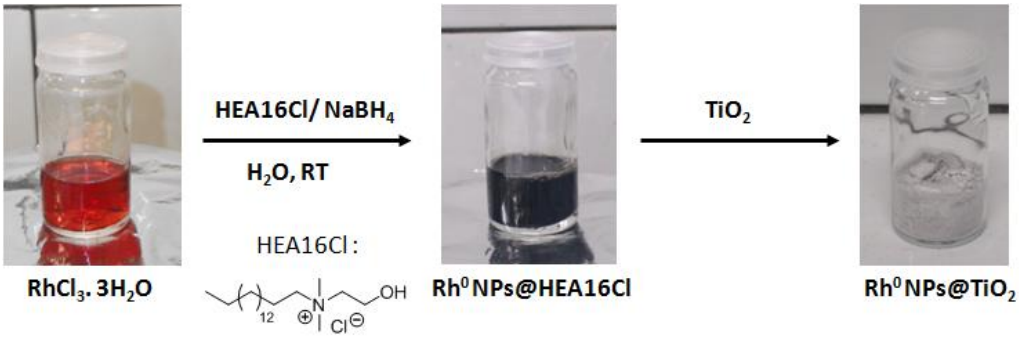


**Figure 2.** One-pot preparation of $Rh^0$ NPs@$TiO_2$ as multicatalytic materials.

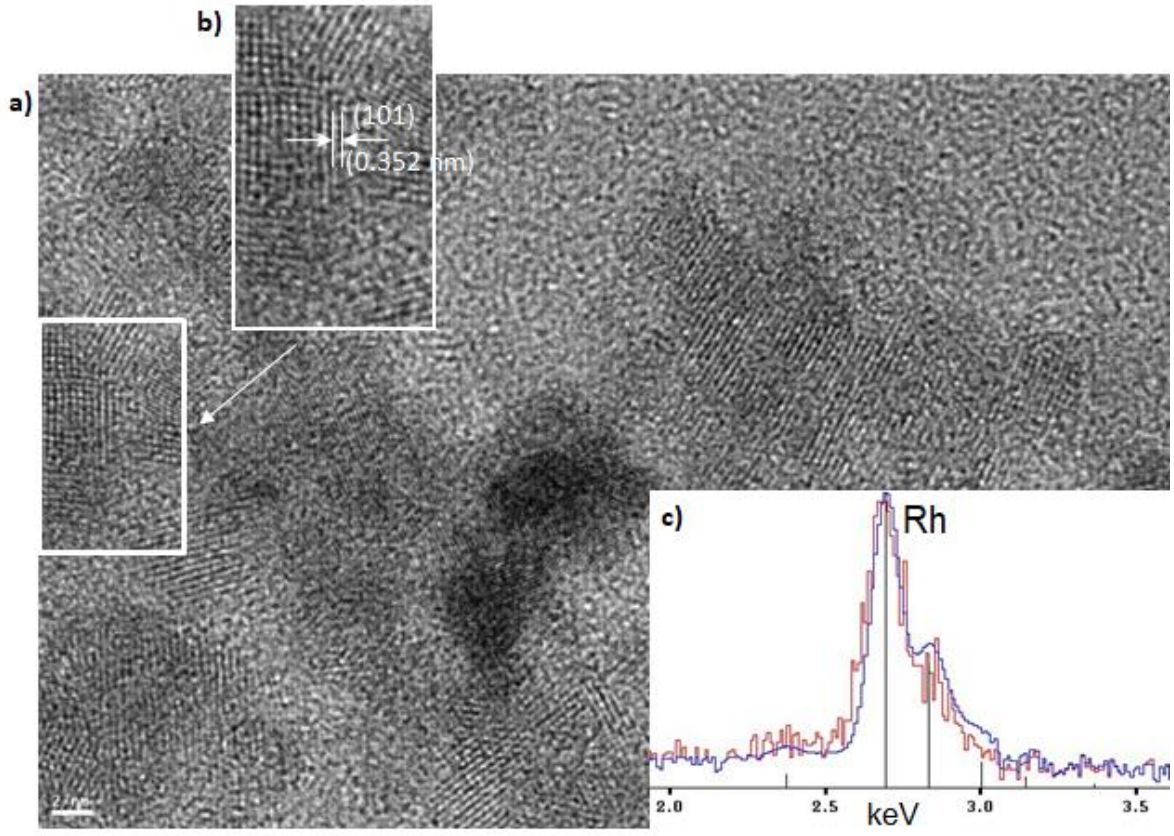


**Figure 3.** HRTEM micrograph. (**a**) Rh(0)NPs@$TiO_2$ (scale bar is 2 nm). (**b**) Magnification of an area showing the lattice planes of $TiO_2$ anatase. (**c**) EDX spectrum of Rh(0) particles proved by deconvolution analysis (red vs. blue curves).

Furthermore, interplanar distances of 0.352 and 0.233 nm, corresponding to the (101) and (112) lattice planes of anatase, were also observed (Figure 3b magnification).

X-ray photoelectron spectroscopy (XPS) measurements were also performed on the multicatalytic materials, to determine the chemical environment of the deposited Rh species (Figure 4). The survey spectra of the Rh(0)NPs@$TiO_2$ catalyst (Figure 4a) contain Ti 2p photoelectron peaks at a binding energy, $E_b$, of 459 eV, and those of O 1s at $E_b$ = 531 eV. The Ti $2p_{1/2}$ and Ti $2p_{3/2}$ spin-orbital splitting photoelectrons are located at binding energies

of 464.6 eV and 459.0 eV, respectively, as observed in Figure 4b. The position of Ti $2p_{3/2}$ is assigned to the presence of a $Ti^{4+}$ oxidation state. The peak separation of 5.596 eV between the Ti $2p_{1/2}$ and Ti $2p_{3/2}$ signals is in good agreement with the reported literature values [59–61]. The O 1s spectrum (Figure 4c) shows a contribution at 530.34 eV, attributed to Ti–O bonds, and a peak at 532.81 eV, which could be assigned to OH groups on the surface [59]. On the other hand, no specific core-level peaks related to N 1s and C 1s, relative to the presence of residual protective surfactant (HEA16Cl), which was used for the NPs stabilization, were observed. These results suggest that the particles were well adsorbed on the support during the wet impregnation methodology, and that the surfactant was totally removed after the washing step. Although double-checked, the Rh species and their 3d peak positions could not be clearly detected by this technique, owing to the very low loading, inferior to 0.1%, as assigned by ICP analysis, but the presence of the Rh species has clearly been assigned by the EDX experiments. Moreover, as indirect proof of the presence of Rh in the catalyst, such $TiO_2$-supported $Rh^0$ nanoparticles have proved to be highly active and reusable in the hydrogenation of mono- or di-substituted and/or functionalized arene derivatives, including chloroanisoles (chloromethoxy benzenes), which were investigated as model substrates for endocrine disruptors [48,55].

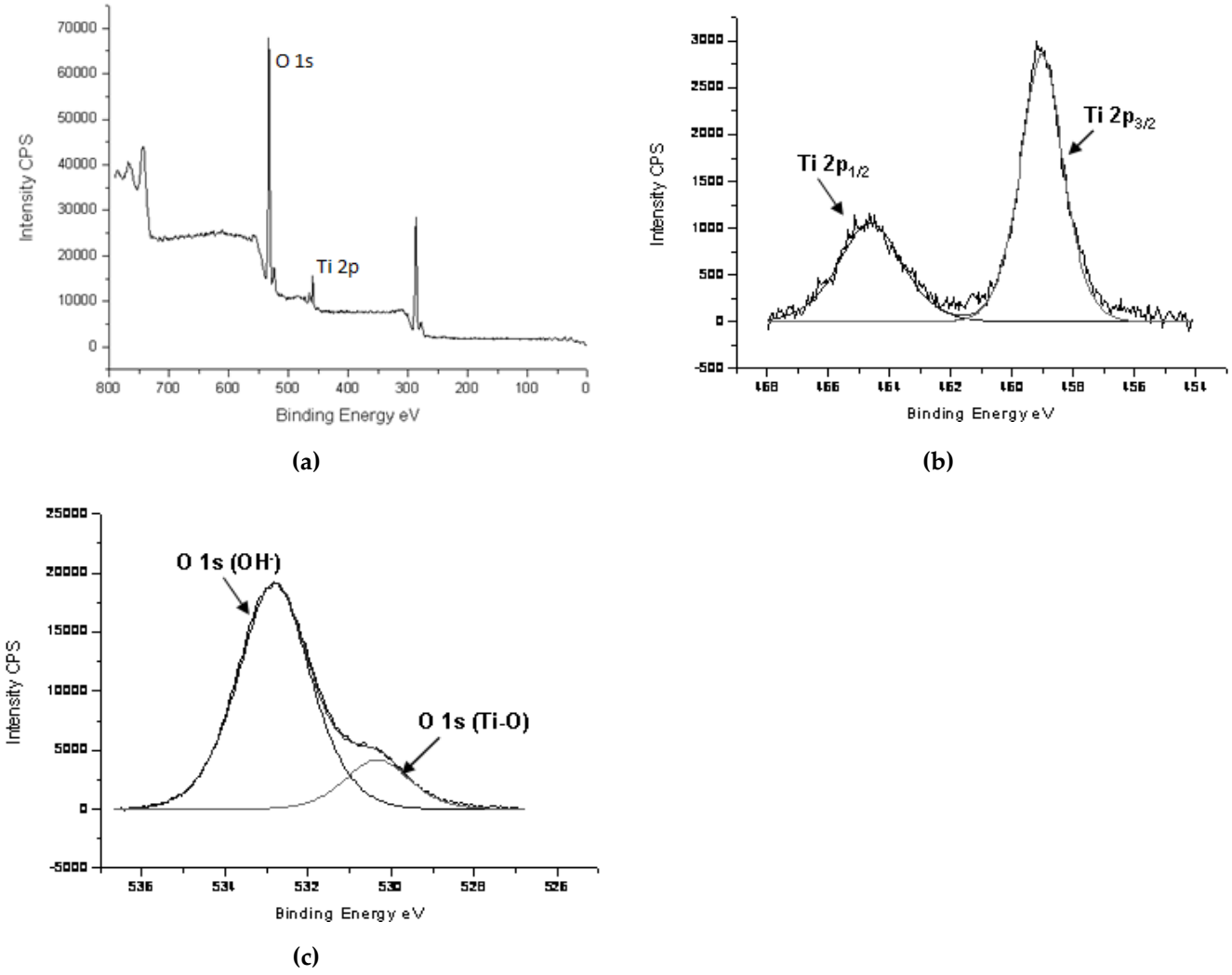


**Figure 4.** X-ray photoelectron spectra of the materials catalyst. (**a**) XPS survey Mg Kα photoelectron spectrum. (**b**) high-resolution XPS spectrum of the Ti 2p peaks. (**c**) High-resolution XPS spectrum of the O 1s peaks.

In the first set of experiments, the photocatalytic activity of the nanocomposite Rh(0)NPs@$TiO_2$ material was investigated in the decomposition of an aqueous solution of diethyl phthalate (DEP), in a 1 mM concentration. The results were compared to the activities of the following three semiconductor materials: (i) the commercial anatase $TiO_2$ from Sigma-Aldrich (99% anatase, 325 mesh); (ii) the commercial rutile $TiO_2$ from Sigma-Aldrich; and (iii) a $TiO_2$ anatase form doped with Au(0) NPs, following the same procedure as for Rh(0) NPs. This Au(0) NPs@$TiO_2$ nanocomposite, with 0.1 wt.% metal loading, was evaluated as a reference, since gold NP-loaded $TiO_2$ materials have already proved their efficiency in the photocatalytic degradation of various pollutants [62,63], owing to their strong visible light absorption, due to localized surface plasmon resonance [64,65]. The aim of this study was to check the effect of rhodium nanospecies on the photoactivity of $TiO_2$ support, and to compare the obtained results to Au doping. Prior to the photodegradation experiments, a series of adsorption tests on the target compound, diethyl phthalate, were performed in the dark, with the different catalytic materials, over 16 h. Whatever the catalyst ($TiO_2$ anatase or rutile forms, Rh(0)NPs@$TiO_2$ or Au(0) NPs@$TiO_2$) was, the adsorption capacities were negligible, with a similar concentration observed after 16 h. These results prove the absence of strong interactions between the substrate and the matrix.

The photocatalytic performances of the Rh(0)NPs@$TiO_2$ as multicatalytic materials for diethyl phthalate photodegradation are presented in Figure 5, and compared to the activities of the commercial anatase and rutile $TiO_2$ polymorphs, and the Au(0)-doped material. First, as a blank experiment, poor degradation was observed in the absence of a catalyst after 6 h with the same concentration. Concerning the $TiO_2$ allotropic forms, as already reported in the literature [66,67], the anatase form presents higher photocatalytic activity than the rutile one, showing a 2 mg·$L^{-1}$ concentration in DEP after only 5 h, while the rutile form led to a 100 mg·$L^{-1}$ ppm concentration after 24 h (Figure 5). Compared with pure anatase $TiO_2$, the photocatalytic efficiencies of the metallic nanoparticle-doped anatase materials (Rh(0)NPs@$TiO_2$ and Au(0)NPs@$TiO_2$) are superior, with a concentration in the endocrine disrupting compound that is inferior to the UV detection limits (<0.2 mg·$L^{-1}$) after 5 h. This result proves the absence of poisonous effects of the active sites, which could have been induced by the presence of zerovalent metallic species at the semi-conductor surface. Moreover, the improved photocatalytic activities, in the case of doped materials, could be explained by an inhibition of electron-hole recombination, owing to the presence of metallic particles at the $TiO_2$ surface, as already reported in the literature, with silver species [68,69] or gold nanoparticles [62,63].

In the second step, since Rh(0) nanoparticles did not disturb the photocatalytic activity of the anatase support, and have already proved to be reference catalysts for the reduction in arene derivatives [55,70], hydrogenation of the endocrine disruptor possessing an aromatic ring was performed as a pre-treatment, to reduce the aromatic structure before photocatalytic degradation. First, the hydrogenation of diethyl phthalate into diethyl hexahydrophthalate was studied at room temperature, and several hydrogen pressures (40, 30, and 1 bar $H_2$) were considered. The results are gathered in Table 1.

**Table 1.** Hydrogenation of diethyl phthalate with Rh(0) NPs@$TiO_2$ nanocatalyst [1].

| Entry | $H_2$ Pressure (Bar) | t (h) | TOF [2] ($h^{-1}$) |
|---|---|---|---|
| 1 [3] | 40 | 0.18 | 1670 |
| 2 | 30 | 0.18 | 1670 |
| 3 | 1 | 3.5 | 90 |

[1] The reaction conditions were as follows: Rh(0)NPs@$TiO_2$ (1g, 0.09 wt.%), diethyl phthalate/metal = 100, 10 mL $H_2O$, room temperature. [2] Turnover frequency defined as the number of $H_2$ mol per mol Rh per hour. [3] Non-optimized.

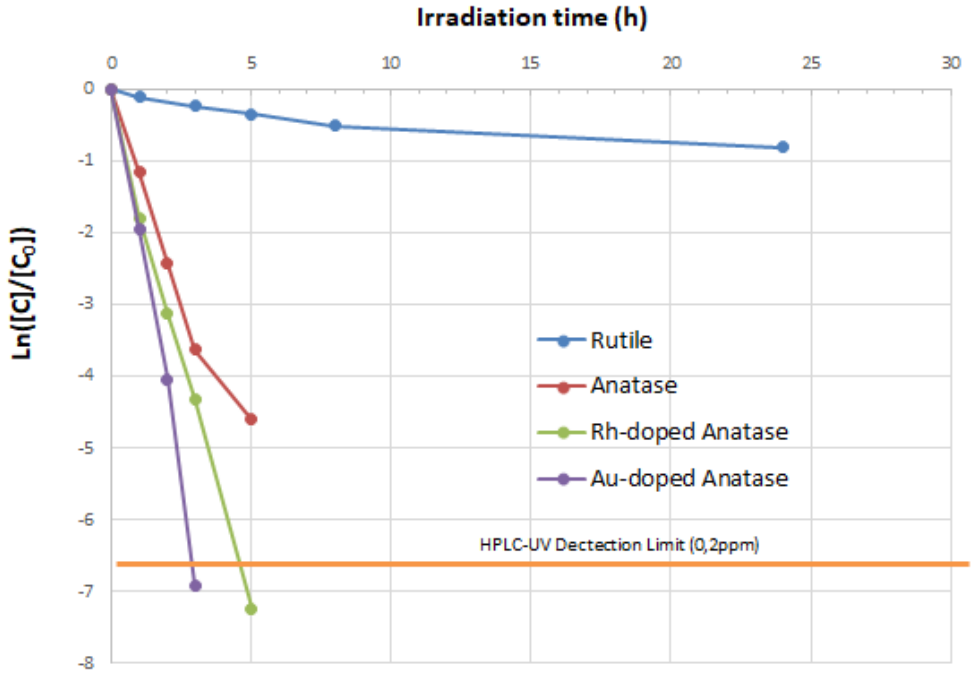


**Figure 5.** Kinetic photodegradation of aqueous diethyl phthalate solution with different catalysts ($TiO_2$ anatase or rutile polymorphs, Rh(0)NPs@$TiO_2$ and Au(0)NPs@$TiO_2$). The reaction conditions were as follows: T = 20 °C, $C_0$ = 222 mg·$L^{-1}$, unregulated pH and an incident light flux of 16 W·$m^{-2}$.

In all cases, the reduction in the aromatic ring is observed with complete conversion in 0.18 to 3.5 h, according to the dihydrogen pressure. A higher turnover frequency of 1670 $h^{-1}$ was achieved under 30 bar $H_2$ (entry 2). The use of milder pressure conditions (atmospheric hydrogen pressure) also leads to the formation of diethyl hexahydrophthalate with a TOF of 90 $h^{-1}$ (entry 3). Moreover, it is worth mentioning that under mild conditions (1 bar $H_2$, room temperature), neither the $TiO_2$ anatase support nor the Au-doped $TiO_2$ material were able to reduce the aromatic ring.

In the final step, photocatalytic remediation of the pre-hydrogenated compound (diethyl hexahydrophthalate) was performed, with the same composite materials as previously described, and was compared with that of diethyl phthalate (Figure 6). Based on previous results on DEP (Figure 5), we presume that the Rh(0)NPs had no negative influence on the photocatalytic activity through a poisoning effect. From the photodegradation curves, higher photoreactivity could be observed for the hydrogenated diethyl phthalate, showing the pertinence of this "domino" process. More than 99% of an aqueous solution of diethyl hexahydrophthalate (222 mg·$L^{-1}$) was rapidly transformed in 2 h, compared to 5 h for diethyl phthalate.

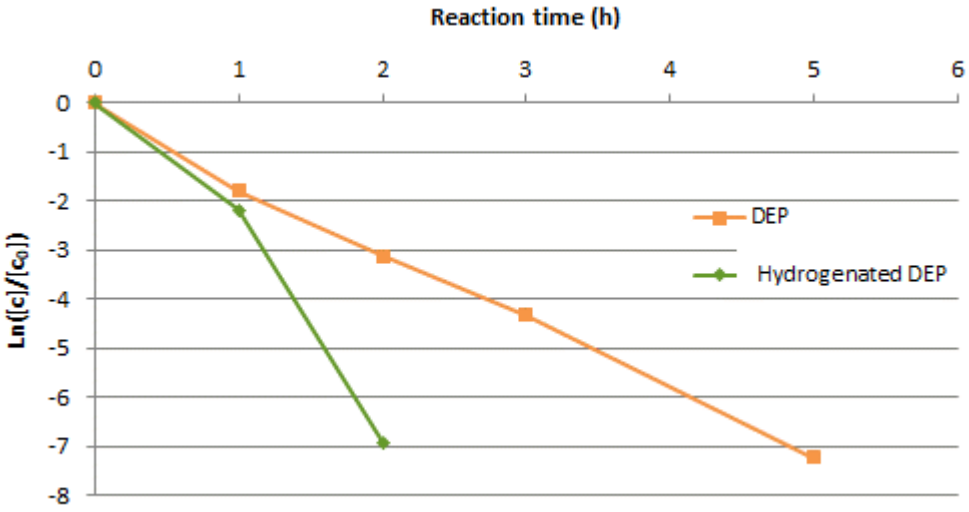


**Figure 6.** Photodegradation of diethyl phthalate and pre-hydrogenated diethyl phthalate in aqueous solution in the presence of $Rh^0$ NPs@$TiO_2$. The reaction conditions were as follows: T = 20 °C, $C_0$ = 222 mg·$L^{-1}$, unregulated pH and an incident light flux of 16 W·$m^{-2}$.

## 3. Materials and Methods

### *3.1. General*

$RhCl_3.3H_2O$ and $HAuCl_4.3H_2O$ were obtained from Strem Chemicals (Bischheim, France). All the organic compounds were purchased from Acros Organics (Illkirch, France) or Sigma-Aldrich-Fluka (Saint-Quentin-Fallavier, France) and used without further purification. The titania anatase and rutile allotropic forms were obtained from Sigma-Aldrich (Saint-Quentin-Fallavier, France). Water was distilled twice before use by conventional method. The *N*,*N*-dimethyl-*N*-cetyl-*N*-(2-hydroxyethyl) ammonium chloride (HEA16Cl) used as a protective agent for the metallic NPs in aqueous solution, was synthesized as previously described in the literature and fully characterized [56,71]. All gas chromatography analyses for catalytic hydrogenation reactions were performed using a Carlo Erba GC 6000 (Val de Reuil, France) with an FID detector equipped with a Thermo Fisher TR-5 (Illkirch, France) column (30 m, 0.25 mm i.d.).

### *3.2. Preparation of Metal NPs@$TiO_2$*

The catalyst was prepared according to a previously described methodology [48]. Titania (19 g) in deionized water (40 mL) was stirred vigorously for two hours. Furthermore, 50 mL of HEA16Cl surfactant-stabilized suspension ($1.9 \times 10^{-4}$ mol of metallic NPs, 2 equiv. of HEA16Cl) were added under vigorous stirring. The system was kept under stirring for two hours. After filtration and three consecutive water washing steps, the grey powder was dried overnight at 60 °C and in air. The ICP analysis gave a metal loading around 0.09%.

### *3.3. General Procedure for Hydrogenation under Atmospheric Hydrogen Pressure*

Reactions were carried out under standard conditions (20 °C, 1 bar $H_2$). A 25 mL round-bottom flask, charged with Rh(0)NPs@$TiO_2$ catalyst (1 g in 10 mL of water) and a magnetic stirrer, was connected with a gas burette (500 mL) to a flask to balance the pressure. The flask was closed by a septum and the system was filled with hydrogen. The diethyl phthalate ([Substrate]/[Metal] = 100) was injected through the septum and the mixture was stirred at 1700 $min^{-1}$. The reaction was monitored by gas chromatography analyses.

### *3.4. General Procedure for Hydrogenation under Hydrogen Pressure*

The stainless-steel autoclave was charged with the Rh(0)NPs@$TiO_2$ catalyst (1 g in 10 mL of water) and a magnetic stirrer. The diethyl phthalate ([Substrate]/[Metal] = 100) was added into the autoclave and dihydrogen was admitted to the system at constant pressure (up to 40 bars). The conversion was determined by gas chromatography analyses. Based on the amount of introduced rhodium, the TOFs values were calculated.

### *3.5. Photocatalytic Experiments*

Irradiations were performed in a cylindrical magnetically stirred batch reactor (volume: V = 4 L, diameter = 18 cm), fitted with a 25 W low-pressure fluorescent lamp (Philips PL-L 24W/10/4P, maximal emission wavelength 365 nm) placed vertically in a plugged tube. The water thickness between the tube and the inner wall was 0.05 m. The radiant flux received by the solution was measured by means of a chemical actinometer (potassium ferrioxalate), which was irradiated under similar conditions to those used during the degradation studies. The incident photon flux was estimated as (8.1 $\pm$ 0.1) $10^{-6}$ Einstein·$s^{-1}$. Further, 222 mg of diethyl phthalate was stirred in 1 L of ultra-pure water for 2 h at room temperature. Then, the aqueous solution was introduced in the photocatalytic reactor with the desired amount of catalyst. Purified air was continuously bubbled into the suspension throughout the experiment and a magnetic stirrer was used to ensure good solid–liquid mixing in the reactor. During each run, samples were taken from the reactor at different irradiation time intervals and filtered to remove the catalyst with a Minisart filter (Sartorius, 0.45 μm). DEP analyses were conducted by HPLC-UV-MS, using a Shimadzu LCMS-2020 UPLC coupled to a simple quadrupole mass spectrometer. The column used was a Thermo Scientific Accucore C18 column (150 mm$\times$ 4.6 mm i.d. with 2.6 μm particle size). The analyses were carried out with a flow rate of 0.5 mL·$mn^{-1}$, with a binary mobile phase composed of acetonitrile acidified with 0.1% formic acid (50%) and ultra-pure water (50%). The detection was performed by mass spectrometry with 1.4 kV tension with an m/z scan ranging from 150 to 550. The selected ion monitoring was adapted to the substrates ($[M+H]^+$ = 223 or 229, respectively, for diethyl phthalate and diethyl hexahydrophthalate).

### *3.6. Adsorption Experiments*

Dark adsorption experiments of both compounds (DEP and hydrogenated DEP) on the photocatalytic media were carried out by mixing aqueous solution of the target compound with the desired amount of catalyst, at 20 $\pm$ 2 °C. The reaction mixture was stirred for 16 h before HPLC-UV-MS analyses.

### *3.7. Transmission Electron Microscopy (TEM) Analysis*

After embedding of the sample in a resin (AGAR 100) and treatment at 70 °C for 48 h for polymerization, the solid was cut into ultrathin lamellas (70 nm) with a diamond knife (Leica Ultracut UCT, Nanterre, France). A TEM analysis was then realized after deposition of the lamellas onto a carbon-covered copper grid using a microscope operating at 200 kV with a resolution of 0.18 nm (JEOL JEM 2011 UHR) equipped with an EDX system (PGT IMX-PC).

### *3.8. X-ray Photoelectron Spectroscopy Analysis*

XPS measurements were performed with a Mg K X-ray source (hv = 1254 eV), using a VSW HA100 photoelectron spectrometer with a hemispherical photoelectron analyzer, working at an energy pass of 22 eV. The experimental resolution was then 1.0 eV. The binding energy for the main C–C peak was taken at 285.0 eV as an internal reference level for all measurements. Spectral analysis included a Shirley background subtraction and peak separation using mixed Gaussian–Lorentzian functions.

## 4. Conclusions

In conclusion, we demonstrated the efficiency of a "domino" process for the remediation of diethyl phthalate, a frequently observed aromatic endocrine disrupting compound in aquatic environments. This original process relies on the use of a single nanocomposite material in two combined reactions, the hydrogenation of the aromatic structure, followed by its photocatalytic degradation, without modification of its structure and properties. This innovative approach, based on multicatalytic materials, could also be very pertinent and promising for photoresistive compounds, at high concentrations, in aqueous effluents. In the process, the rhodium (0) nanoparticles, which were active in arene hydrogenation, were immobilized on $TiO_2$ anatase, a well-known photoactive support, offering the opportunity to use a unique catalyst for these successive steps. This multi-site nanocatalyst was easily prepared in the absence of organic solvent and a calcination step, and is highly active, even at very low Rh loading, without any leaching during the catalytic process. Further works are ongoing to combine reactions in the same reactor, to optimize manipulation as well as the reaction time, and, finally, to determine the intermediates, and thus propose a degradation pathway for 1,2-diethylphthalate. Although the scope of this work is limited to a laboratory scale for diethyl phthalate remediation, this efficient and environmentally friendly "domino" approach constitutes a promising alternative, particularly for the removal of pollutants, which are refractory to classical oxidative processes.

**Author Contributions:** Investigation: C.-H.P.; Formal analysis: I.S.; Photocatalytic methodology: L.F.; Conceptualization, writing—review and editing: A.R. and A.D.-N. All authors have read and agreed to the published version of the manuscript.

**Funding:** This research was funded by the Region Bretagne (Ph.D. Grant of C. Hubert and C.-H. Pélisson) as well as the Institut des Sciences Chimiques de Rennes (UMR 6226) for the financial support of both ENSCR teams.

**Data Availability Statement:** The data that support the findings of this study are available from the corresponding author upon reasonable request.

**Acknowledgments:** The authors are grateful to the Region Bretagne for Ph.D. Grant of C. Hubert and C.-H. Pélisson as well as the Institut des Sciences Chimiques de Rennes (UMR 6226) for the financial support of both ENSCR teams. The authors are indebted to Patricia Beaunier from the Service de Microscopie Electronique at Sorbonne Universités UPMC for Transmission Electron Microscopy analyses.

**Conflicts of Interest:** The authors declare no conflict of interest.

## References

1. Gómez-Hens, A.; Aguilar-Caballos, M. Social and economic interest in the control of phthalic acid esters. *TrAC Trends Anal. Chem.* **2003**, *22*, 847–857. [CrossRef]
2. Prasad, B. Phthalate pollution: Environmental fate and cumulative human exposure index using the multivariate analysis approach. *Environ. Sci. Process. Impacts* **2021**, *23*, 389–399. [CrossRef] [PubMed]
3. Bergé, A.; Cladière, M.; Gasperi, J.; Coursimault, A.; Tassin, B.; Moilleron, R. Meta-analysis of environmental contamination by phthalates. *Environ. Sci. Pollut. Res.* **2013**, *20*, 8057–8076. [CrossRef] [PubMed]
4. Wu, Y.; Sun, J.; Zheng, C.; Zhang, X.; Zhang, A.; Qi, H. Phthalate pollution driven by the industrial plastics market: A case study of the plastic market in Yuyao City, China. *Environ. Sci. Pollut. Res.* **2019**, *26*, 11224–11233. [CrossRef]
5. Staples, C.A.; Peterson, D.R.; Parkerton, T.F.; Adams, W.J. The environmental fate of phthalate esters: A literature review. *Chemosphere* **1997**, *35*, 667–749. [CrossRef]
6. Jobling, S.; Reynolds, T.; White, R.; Parker, M.G.; Sumpter, J.P. A variety of environmentally persistent chemicals, including some phthalate plasticizers, are weakly estrogenic. *Environ. Health Perspect.* **1995**, *103*, 582–587. [CrossRef]
7. Van Wezel, A.; Van Vlaardingen, P.; Posthumus, R.; Crommentuijn, G.; Sijm, D. Environmental Risk Limits for Two Phthalates, with Special Emphasis on Endocrine Disruptive Properties. *Ecotoxicol. Environ. Saf.* **2000**, *46*, 305–321. [CrossRef]
8. Wittassek, M.; Angerer, J.; Kolossa-Gehring, M.; Schäfer, S.D.; Klockenbusch, W.; Dobler, L.; Günsel, A.K.; Müller, A.; Wiesmüller, G.A. Fetal exposure to phthalates—A pilot study. *Int. J. Hyg. Environ. Health* **2009**, *212*, 492–498. [CrossRef]
9. Peng, X.; Feng, L.; Li, X. Pathway of diethyl phthalate photolysis in sea-water determined by gas chromatography–mass spectrometry and compound-specific isotope analysis. *Chemosphere* **2013**, *90*, 220–226. [CrossRef]

10. Liang, D.; Zhang, T.; Fang, H.H.P.; He, J. Phthalates biodegradation in the environment. *Appl. Microbiol. Biotechnol.* **2008**, *80*, 183–198. [CrossRef]
11. Perpetuo, E.A.; da Silva, E.C.N.; Karolski, B.; do Nascimento, C.A.O. Biodegradation of diethyl-phthalate (DEP) by halo-tolerant bacteria isolated from an estuarine environment. *Biodegradation* **2020**, *31*, 331–340. [CrossRef] [PubMed]
12. Shaida, M.A.; Dutta, R.; Sen, A. Removal of diethyl phthalate via adsorption on mineral rich waste coal modified with chitosan. *J. Mol. Liq.* **2018**, *261*, 271–282. [CrossRef]
13. Alves, D.D.S.; Healy, B.; Pinto, L.; Cadaval, T.; Breslin, C. Recent Developments in Chitosan-Based Adsorbents for the Removal of Pollutants from Aqueous Environments. *Molecules* **2021**, *26*, 594. [CrossRef]
14. Guo, R.; Yan, L.; Rao, P.; Wang, R.; Guo, X. Nitrogen and sulfur co-doped biochar derived from peanut shell with en-hanced adsorption capacity for diethyl phthalate. *Environ. Pollut.* **2020**, *258*, 113674. [CrossRef]
15. Cesaro, V.; Belgiorno, V. Removal of Endocrine Disruptors from Urban Wastewater by Advanced Oxidation Processes (AOPs): A Review. *Open Biotechnol. J.* **2016**, *10*, 151–172. [CrossRef]
16. Mansouri, L.; Sabelfeld, M.; Geissen, S.-U.; Bousselmi, L. Catalytic ozonation of model organic compounds in aqueous solution promoted by metallic oxides. *Desalin. Water Treat.* **2015**, *53*, 1089–1100. [CrossRef]
17. Zammit, I.; Vaiano, V.; Ribeiro, A.R.; Silva, A.M.T.; Manaia, C.M.; Rizzo, L. Immobilised Cerium-Doped Zinc Oxide as a Photocatalyst for the Degradation of Antibiotics and the Inactivation of Antibiotic-Resistant Bacteria. *Catalysts* **2019**, *9*, 222. [CrossRef]
18. Liang, D.; Zhang, T.; Fang, H.H. Anaerobic degradation of dimethyl phthalate in wastewater in a UASB reactor. *Water Res.* **2007**, *41*, 2879–2884. [CrossRef]
19. Roslev, P.; Vorkamp, K.; Aarup, J.; Frederiksen, K.; Nielsen, P.H. Degradation of phthalate esters in an activated sludge wastewater treatment plant. *Water Res.* **2007**, *41*, 969–976. [CrossRef]
20. Medellin-Castillo, N.A.; Ocampo-Pérez, R.; Leyva-Ramos, R.; Sanchez-Polo, M.; Rivera-Utrilla, J.; Méndez-Díaz, J.D. Removal of diethyl phthalate from water solution by adsorption, photo-oxidation, ozonation and advanced oxidation process ($UV/H_2O_2$, $O_3/H_2O_2$ and $O_3$/activated carbon). *Sci. Total Environ.* **2013**, *442*, 26–35. [CrossRef]
21. Mansouri, L.; Tizaoui, C.; Geissen, S.-U.; Bousselmi, L. A comparative study on ozone, hydrogen peroxide and UV based advanced oxidation processes for efficient removal of diethyl phthalate in water. *J. Hazard. Mater.* **2019**, *363*, 401–411. [CrossRef]
22. Zhao, H.; Wang, Q.; Chen, Y.; Tian, Q.; Zhao, G. Efficient removal of dimethyl phthalate with activated iron-doped carbon aerogel through an integrated adsorption and electro-Fenton oxidation process. *Carbon* **2017**, *124*, 111–122. [CrossRef]
23. Wang, X.; Ding, Y.; Dionysiou, D.D.; Liu, C.; Tong, Y.; Gao, J.; Fang, G.; Zhou, D. Efficient activation of peroxymonosulfate by copper sulfide for diethyl phthalate degradation: Performance, radical generation and mechanism. *Sci. Total. Environ.* **2020**, *749*, 142387. [CrossRef] [PubMed]
24. Xu, B.; Gao, N.-Y.; Sun, X.-F.; Xia, S.; Rui, M.; Simonnot, M.-O.; Causserand, C.; Zhao, J.-F. Photochemical degradation of diethyl phthalate with $UV/H_2O_2$. *J. Hazard. Mater.* **2007**, *139*, 132–139. [CrossRef] [PubMed]
25. De Oliveira, T.F.; Cagnon, B.; Chedeville, O.; Fauduet, H. Removal of a mix of endocrine disrupters from different natural matrices by ozone/activated carbon coupling process. *Desalination Water Treat.* **2013**, *52*, 4395–4403. [CrossRef]
26. Mohan, S.; Mamane, H.; Avisar, D.; Gozlan, I.; Kaplan, A.; Dayalan, G. Treatment of Diethyl Phthalate Leached from Plastic Products in Municipal Solid Waste Using an Ozone-Based Advanced Oxidation Process. *Materials* **2019**, *12*, 4119. [CrossRef]
27. Wen, G.; Wang, S.-J.; Ma, J.; Huang, T.-L.; Liu, Z.-Q.; Zhao, L.; Su, J.-F. Enhanced ozonation degradation of di-n-butyl phthalate by zero-valent zinc in aqueous solution: Performance and mechanism. *J. Hazard. Mater.* **2014**, *265*, 69–78. [CrossRef] [PubMed]
28. Wang, J.; Cheng, J.; Wang, C.; Yang, S.; Zhu, W. Catalytic ozonation of dimethyl phthalate with $RuO_2/Al_2O_3$ catalysts prepared by microwave irradiation. *Catal. Commun.* **2013**, *41*, 1–5. [CrossRef]
29. Ruiz, J.A.; Rodríguez, J.L.; Poznyak, T.; Chairez, I.; Dueñas, J. Catalytic effect of $\gamma$-$Al(OH)_3$, $\alpha$-FeOOH, and $\alpha$-$Fe_2O_3$ on the ozonation-based decomposition of diethyl phthalate adsorbed on sand and soil. *Environ. Sci. Pollut. Res.* **2021**, *28*, 974–981. [CrossRef]
30. Klavarioti, M.; Mantzavinos, D.; Kassinos, D. Removal of residual pharmaceuticals from aqueous systems by advanced oxidation processes. *Environ. Int.* **2009**, *35*, 402–417. [CrossRef]
31. Chong, M.N.; Jin, B.; Chow, C.W.K.; Saint, C. Recent developments in photocatalytic water treatment technology: A review. *Water Res.* **2010**, *44*, 2997–3027. [CrossRef]
32. Sin, J.C.; Lam, S.M.; Mohamed, A.R.; Lee, K.T. Degrading endocrine disrupting chemicals from wastewater by $TiO_2$ photocatalysis: A review. *Int. J. Photoenergy* **2012**, *2012*, 185159. [CrossRef]
33. Al-Madanat, O.; AlSalka, Y.; Ramadan, W.; Bahnemann, D. $TiO_2$ Photocatalysis for the Transformation of Aromatic Water Pollutants into Fuels. *Catalysts* **2021**, *11*, 317. [CrossRef]
34. Mashuri, S.I.S.; Ibrahim, M.L.; Kasim, M.F.; Mastuli, M.S.; Rashid, U.; Abdullah, A.H.; Islam, A.; Mijan, N.A.; Tan, Y.H.; Mansir, N.; et al. Photocatalysis for Organic Wastewater Treatment: From the Basis to Current Challenges for Society. *Catalysts* **2020**, *10*, 1260. [CrossRef]
35. Malato, S.; Fernández-Ibáñez, P.; Maldonado, M.I.; Blanco, J.; Gernjak, W. Decontamination and disinfection of water by solar photocatalysis: Recent overview and trends. *Catal. Today* **2009**, *147*, 1–59. [CrossRef]
36. Hoffmann, M.R.; Martin, S.T.; Choi, W.; Bahnemann, D.W. Environmental Applications of Semiconductor Photocatalysis. *Chem. Rev.* **1995**, *95*, 69–96. [CrossRef]

37. Muneer, M.; Theurich, J.; Bahnemann, D.B.D. Titanium dioxide mediated photocatalytic degradation of 1,2-diethyl phthalate. *J. Photochem. Photobiol. A Chem.* **2001**, *143*, 213–219. [CrossRef]
38. Huang, W.-B.; Chen, C.-Y. Photocatalytic Degradation of Diethyl Phthalate (DEP) in Water Using $TiO_2$. *Water Air Soil Pollut.* **2009**, *207*, 349–355. [CrossRef]
39. Ding, X.; An, T.; Li, G.; Chen, J.; Sheng, G.; Fu, J.; Zhao, J. Photocatalytic degradation of dimethyl phthalate ester using nov-el hydrophobic $TiO_2$ pillared montmorillonite photocatalyst. *Res. Chem. Intermediat.* **2008**, *34*, 67–83. [CrossRef]
40. Chang, C.-F.; Man, C.-Y. Titania-Coated Magnetic Composites as Photocatalysts for Phthalate Photodegradation. *Ind. Eng. Chem. Res.* **2011**, *50*, 11620–11627. [CrossRef]
41. Chalasani, R.; Vasudevan, S. Cyclodextrin-Functionalized $Fe_3O_4$@$TiO_2$: Reusable, Magnetic Nanoparticles for Photocatalytic Degradation of Endocrine-Disrupting Chemicals in Water Supplies. *ACS Nano* **2013**, *7*, 4093–4104. [CrossRef]
42. Chen, Q.; Shi, H.; Shi, W.; Xu, Y.; Wu, D. Enhanced visible photocatalytic activity of titania–silica photocatalysts: Effect of carbon and silver doping. *Catal. Sci. Technol.* **2012**, *2*, 1213–1220. [CrossRef]
43. Singla, P.; Pandey, O.P.; Singh, K. Study of photocatalytic degradation of environmentally harmful phthalate esters using Ni-doped TiO2 nanoparticles. *Int. J. Environ. Sci. Technol.* **2015**, *13*, 849–856. [CrossRef]
44. Ki, S.J.; Park, Y.-K.; Kim, J.-S.; Lee, W.-J.; Lee, H.; Jung, S.-C. Facile preparation of tungsten oxide doped TiO2 photocatalysts using liquid phase plasma process for enhanced degradation of diethyl phthalate. *Chem. Eng. J.* **2019**, *377*, 120087. [CrossRef]
45. Narayan, N.; Meiyazhagan, A.; Vajtai, R. Metal Nanoparticles as Green Catalysts. *Materials* **2019**, *12*, 3602. [CrossRef] [PubMed]
46. Denicourt-Nowicki, A.; Roucoux, A. Odyssey in Polyphasic Catalysis by Metal Nanoparticles. *Chem. Rec.* **2016**, *16*, 2127–2141. [CrossRef] [PubMed]
47. Denicourt-Nowicki, A.; Mordvinova, N.; Roucoux, A. Metal nanoparticles in water: A relevant toolbox for green catalysis. In *Nanoparticles in Catalysis. Advances in Synthesis and Applications*; Philippot, K., Roucoux, A., Eds.; Wiley-VCH: Weinheim, Germany, 2021; pp. 45–71.
48. Hubert, C.; Denicourt-Nowicki, A.; Beaunier, P.; Roucoux, A. $TiO_2$-supported Rh nanoparticles: From green catalyst preparation to application in arene hydrogenation in neat water. *Green Chem.* **2010**, *12*, 1167–1170. [CrossRef]
49. Heuson, E.; Dumeignil, F. The various levels of integration of chemo- and bio-catalysis towards hybrid catalysis. *Catal. Sci. Technol.* **2020**, *10*, 7082–7100. [CrossRef]
50. Hubert, C.; Bilé, E.G.; Denicourt-Nowicki, A.; Roucoux, A. Tandem dehalogenation–hydrogenation reaction of halogenoarenes as model substrates of endocrine disruptors in water: Rhodium nanoparticles in suspension vs. on silica support. *Appl. Catal. A Gen.* **2011**, *394*, 215–219. [CrossRef]
51. Tan, B.L.; Hawker, D.W.; Müller, J.F.; Leusch, F.; Tremblay, L.; Chapman, H.F. Modelling of the fate of selected endocrine disruptors in a municipal wastewater treatment plant in South East Queensland, Australia. *Chemosphere* **2007**, *69*, 644–654. [CrossRef]
52. Tan, G.H. Residue levels of phthalate esters in water and sediment samples from the Klang River basin. *Bull. Environ. Contam. Toxicol.* **1995**, *54*, 171–176. [CrossRef]
53. Staples, C.A.; Parkerton, T.F.; Peterson, D.R. A risk assessment of selected phthalate esters in North American and West-ern European surface waters. *Chemosphere* **2000**, *40*, 885–891. [CrossRef]
54. Gani, K.M.; Tyagi, V.K.; Kazmi, A.A. Occurrence of phthalates in aquatic environment and their removal during wastewater treatment processes: A review. *Environ. Sci. Pollut. Res.* **2017**, *24*, 17267–17284. [CrossRef]
55. Hubert, C.; Bilé, E.G.; Denicourt-Nowicki, A.; Roucoux, A. Rh(0) colloids supported on $TiO_2$: A highly active and pertinent tandem in neat water for the hydrogenation of aromatics. *Green Chem.* **2011**, *13*, 1766–1771. [CrossRef]
56. Bilé, E.G.; Sassine, R.; Denicourt-Nowicki, A.; Launay, F.; Roucoux, A. New ammonium surfactant-stabilized rho-dium(0) colloidal suspensions: Influence of novel counter-anions on physico-chemical and catalytic properties. *Dalton Trans.* **2011**, *40*, 6524–6531. [CrossRef]
57. Barthe, L.; Hemati, M.; Philippot, K.; Chaudret, B.; Denicourt-nowicki, A.; Roucoux, A. Rhodium colloidal suspension deposition on porous silica particles by dry impregnation: Study of the influence of the reaction conditions on nanoparticles loca-tion and dispersion and catalytic reactivity. *Chem. Eng. J.* **2009**, *151*, 372–379. [CrossRef]
58. Pélisson, C.-H.; Hubert, C.; Denicourt-Nowicki, A.; Roucoux, A. From Hydroxyalkylammonium Salts to Protected-Rh(0) Nanoparticles for Catalysis in Water: Comparative Studies of the Polar Heads. *Top. Catal.* **2013**, *56*, 1220–1227. [CrossRef]
59. Pouilleau, J.; Devilliers, D.; Groult, H.; Marcus, P. Surface study of a titanium-based ceramic electrode material by X-ray photoelectron spectroscopy. *J. Mater. Sci.* **1997**, *32*, 5645–5651. [CrossRef]
60. McCafferty, E.; Wightman, J.P. Determination of the concentration of surface hydroxyl groups on metal oxide films by a quantitative XPS method. *Surf. Interface Anal.* **1998**, *26*, 549–564. [CrossRef]
61. Erdem, B.; Hunsicker, R.A.; Simmons, G.W.; Sudol, E.D.; Dimonie, V.L.; El-Aasser, M.S. XPS and FTIR Surface Characterization of $TiO_2$ Particles Used in Polymer Encapsulation. *Langmuir* **2001**, *17*, 2664–2669. [CrossRef]
62. Naya, S.-I.; Nikawa, T.; Kimura, K.; Tada, H. Rapid and Complete Removal of Nonylphenol by Gold Nanoparticle/Rutile Titanium(IV) Oxide Plasmon Photocatalyst. *ACS Catal.* **2013**, *3*, 903–907. [CrossRef]
63. Pugazhenthiran, N.; Murugesan, S.; Sathishkumar, P.; Anandan, S. Photocatalytic degradation of ceftiofur sodium in the presence of gold nanoparticles loaded TiO2 under UV–visible light. *Chem. Eng. J.* **2014**, *241*, 401–409. [CrossRef]

64. Pelaez, M.; Nolan, N.T.; Pillai, S.C.; Seery, M.K.; Falaras, P.; Kontos, A.G.; Dunlop, P.S.M.; Hamilton, J.W.J.; Byrne, J.A.; O'Shea, K.; et al. A review on the visible light active titanium dioxide photocatalysts for environmen-tal applications. *Appl. Catal. B* **2012**, *125*, 331–349. [CrossRef]
65. Hussain, M.; Ahmad, M.; Nisar, A.; Sun, H.; Karim, S.; Khan, M.; Khan, S.D.; Iqbal, M.; Hussain, S.Z. Enhanced photocatalytic and electrochemical properties of Au nanoparticles supported $TiO_2$ microspheres. *New J. Chem.* **2014**, *38*, 1424–1432. [CrossRef]
66. Liu, L.; Zhao, H.; Andino, J.M.; Li, Y. Photocatalytic $CO_2$ Reduction with $H_2O$ on $TiO_2$ Nanocrystals: Comparison of Anatase, Rutile, and Brookite Polymorphs and Exploration of Surface Chemistry. *ACS Catal.* **2012**, *2*, 1817–1828. [CrossRef]
67. Luttrell, T.; Halpegamage, S.; Tao, J.; Kramer, A.; Sutter, E.A.; Batzill, M. Why is anatase a better photocatalyst than rutile?—Model studies on epitaxial TiO2 films. *Sci. Rep.* **2014**, *4*, 4043. [CrossRef] [PubMed]
68. Hirakawa, T.; Kamat, P.V. Charge Separation and Catalytic Activity of Ag@$TiO_2$ Core—Shell Composite Clusters under UV—Irradiation. *J. Am. Chem. Soc.* **2005**, *127*, 3928–3934. [CrossRef]
69. Ji, Z.; Ismail, M.N.; Callahan, D.M.; Pandowo, E.; Cai, Z.; Goodrich, T.L.; Ziemer, K.S.; Warzywoda, J.; Sacco, A. The role of silver nanoparticles on silver modified titanosilicate ETS-10 in visible light photocatalysis. *Appl. Catal. B Environ.* **2011**, *102*, 323–333. [CrossRef]
70. Chacon, G.; Dupont, J. Arene Hydrogenation by Metal Nanoparticles in Ionic Liquids. *ChemCatChem* **2019**, *11*, 333–341. [CrossRef]
71. Schulz, J.; Roucoux, A.; Patin, H. Stabilized Rhodium(0) Nanoparticles: A Reusable Hydrogenation Catalyst for Arene Derivatives in a Biphasic Water-Liquid System. *Chem. Eur. J.* **2000**, *6*, 618–624. [CrossRef]